

***Final Draft***  
**of the original manuscript:**

Tarazona, N.; Machatschek, R.; Lendlein, A.:  
**Unraveling the interplay between abiotic hydrolytic degradation and  
crystallization of bacterial polyesters comprising short and medium side-  
chain length polyhydroxyalkanoates.**  
In: *Biomacromolecules*. Vol. 21 (2020) 2, 761 - 771.  
First published online by ACS: 16.12.2019

DOI: 10.1021/acs.biomac.9b01458  
<https://dx.doi.org/10.1021/acs.biomac.9b01458>

# Unraveling the interplay between abiotic hydrolytic degradation and crystallization of bacterial polyesters comprising short and medium side-chain length polyhydroxyalkanoates

*Natalia A. Tarazona<sup>†</sup>, Rainhard Machatschek<sup>‡</sup>, and Andreas Lendlein<sup>†,‡,\*</sup>*

<sup>†</sup> Institute of Biomaterial Science and Berlin-Brandenburg Center for Regenerative Therapies,  
Helmholtz-Zentrum Geesthacht, Kantstraße 55, 14513 Teltow, Germany

<sup>‡</sup> Institute of Chemistry, University of Potsdam, Karl-Liebknecht-Straße 24-25, 14469  
Potsdam, Germany

\*Corresponding author:

A. Lendlein, e-mail: [andreas.lendlein@hzg.de](mailto:andreas.lendlein@hzg.de)

## **ABSTRACT**

Polyhydroxyalkanoates (PHAs) attract attention as degradable (co)polyesters which can be produced by microorganisms with variations in the side-chain. This structural variation does not only influence the thermomechanical properties of the material, but also its degradation

behavior. Here, we used Langmuir monolayers at the air–water (A–W) interface as suitable models for evaluating the abiotic degradation of two PHAs with different side-chain lengths and crystallinity. By controlling the polymer state (semi-crystalline, amorphous), the packing density, the pH, and the degradation mechanism, we could draw several significant conclusions. i) The maximum degree of crystallinity for a PHA film to be efficiently degraded up to pH = 12.3 is 40%; ii) PHA made of repeating units with shorter side-chain length are more easily hydrolyzed under alkaline conditions. The efficiency of alkaline hydrolysis decreased by about 65% when the polymer was 40% crystalline iii) in PHA films with a relatively high initial crystallinity, abiotic degradation initiated a chemi-crystallization phenomenon, detected as an increase in the storage modulus ( $E'$ ). This could translate into an increase in brittleness and reduction in the material degradability. Finally, we demonstrate the stability of the measurement system for long-term experiments, which allows degradation conditions for polymers that could closely simulate real-time degradation.

## INTRODUCTION

The interest in degradable polymers that can compete with synthetic polymers in medical applications such as regenerative medicine, has placed bacterial polyhydroxyalkanoates (PHAs) under the spotlight for many years.<sup>1</sup> PHAs are linear and isotactic polyesters composed of (*R*)-hydroxyalkanoic acid building blocks, stored as insoluble cytoplasmic inclusions coated by a surface layer that contains surface-active proteins (PHA granules).<sup>2-4</sup> Using various substrates, a huge variety of PHAs can be synthesized, differing markedly by the length of their side-chains. It has been proposed that PHA's hydrophobic polymer chains exist in a mobile amorphous elastomeric state in native granules (nPHA granules), stabilized by the plasticizing effect of water and the presence of the surfactant-like proteins<sup>5</sup>. Upon extraction from the cell,

or after cell lysis, the surface layer of nPHA granules is damaged or lost and the polyester chains can adopt an ordered helical conformation and develop a crystalline phase.<sup>6</sup> The tendency of the polymers to crystallize depends on the sequence structure. For example, isolated poly(3-*R*-hydroxybutyrate) (PHB) is a semi-crystalline polymer (typical degree of crystallinity 50–60%) with glass transition temperature  $T_g \approx 4$  °C, and a crystalline fraction that melts in the range  $180 \pm 10$  °C.<sup>7</sup> PHA containing repeat units with longer side-chains, such as 3-*R*-hydroxyhexanoate (3HHx), 3-*R*-hydroxyoctanoate (3HO), and 3-*R*-hydroxydecanoate (3HD), usually have lower crystallinities and can even be fully amorphous.<sup>8</sup> In some cases, as in PHA with high percentages of 3-*R*-hydroxydodecanoate (3HDD) or 3-*R*-hydroxytetradecanoate (3HTD), the presence of long side-chains has been shown to increase polymer crystallinity, presumably due to side-chain crystallization.<sup>9</sup>

The biodegradation of PHAs is of great relevance to several fields of application. Their degradation has been studied in several managed (composting) and unmanaged (marine/aquatic conditions and soil) environments.<sup>10</sup> In natural environments like soil, PHA-based materials can be degraded by extracellular depolymerases, which are secreted by a variety of microorganisms ubiquitously present in the ecosystem. These enzymes hydrolyze the water-insoluble (co)polymers to water-soluble fragments, which are then utilized by the microorganisms as carbon and energy sources.<sup>11</sup> Narancic et al. tested the degradation behavior of different PHA nets and blends, simulating specific environmental conditions (biotic degradation) according to ISO standards.<sup>10</sup> Outlined, PHB showed relatively fast degradation rates and reached the standard for biodegradation in the 7 mimicked environments (e.g. industrial composting, soil, aquatic environments). Blends of PHB with poly( $\epsilon$ -caprolactone) exhibited improved biodegradability. Remarkably, amorphous PHO degraded poorly in most of the conditions tested, reaching standard criteria only in industrial composting.<sup>10</sup>

PHA-based medical devices are also expected to degrade in biological environments, such as the human body, and their degradation products are believed to be non-toxic. In fact, 3-hydroxybutyrate, the building block of PHB, is naturally encountered as a physiological metabolite in all higher living beings.<sup>12, 13</sup> In addition, PHAs with no side-chains in the carbon backbone, such as poly(4-hydroxybutyrate) (P4HB), and poly(3-*R*-hydroxypropionate) PHP, are prone to be hydrolyzed by several prokaryotic and eukaryotic lipases.<sup>14, 15</sup> This further supports the biodegradation of PHA-based biomaterials in living systems.

Some PHA (co)polymers have been the subject of experimental studies for the fabrication of devices such as sutures, carrier matrices, and cardiovascular patches.<sup>16-20</sup> However, from the standpoint of medical application development, there is still a lack of accurate methodologies to predict the kinetics and consequences of the degradation of PHA materials, including the effect on their mechanical properties and their crystallinity. This largely relies on the fact that PHAs' extracellular degradation rates are affected by several interdependent factors, which are challenging to control by traditional bulk degradation experiments. For instance: i) the side-chain length of the 3-hydroxyalkanoate repeating units, ii) the difference in phase morphology of the materials as a consequence of variations in sequence structure and preparation method iii) the sample geometry of the PHAs, e.g. film, granule, pellets, iv) and the degradation conditions (pH, temperature, enzymes).<sup>11, 21, 22</sup>

Findings in this matter are confusing and sometimes even contradictory, making it difficult to draw general conclusions on PHA degradation mechanisms, and consequently to expand their application. Therefore, it is essential to understand the molecular mechanism of PHA hydrolytic and enzymatically catalyzed degradation, using a technique that allows studying the degradation of PHA independent of sample geometry while precisely controlling the phase morphology and the external conditions.

In our approach, we use Langmuir monolayers at the air–water (A–W) interface for evaluating PHA hydrolytic degradation, controlling the (co)polymer state (crystalline, amorphous), the pH, and the degradation mechanism. With the Langmuir approach, molecular thin films are formed at the A–W interface with precise control of the area per molecule and other experimental conditions, permitting the investigation of polymer properties/functions with a two-dimensional model system.<sup>23</sup> When degradable polymer thin films at the A–W interface form water-soluble degradation products, the concentration of chain segments at the surface decreases, leading to a decline of the surface pressure, measured by a surface tension sensor coupled to the Langmuir trough. By keeping the surface pressure, and thereby the areal concentration of chain segments constant, the area of the film reduces, and the area reduction is proportional to the mass loss of the film.<sup>24</sup> Langmuir Monolayer Degradation experiments (LMD) are combined with *in situ* interfacial rheology to detect the alterations in the mechanical properties of the (co)polymer layers.

In this manuscript, we compare two semi-crystalline and isotactic PHAs with different sequence structure. PHB is the most studied PHA homo-polymer, consisting of 3-*R*-hydroxybutyrate repeating units (methyl group as a side-chain). As bulk material PHB is brittle and has high melting points. The glass transition temperature ( $T_g$ ), the crystallization temperature ( $T_{cc}$ ) and the melting temperature ( $T_m$ ) of PHB, measured by Differential Scanning Calorimetry (DSC), have been reported to be  $5 \pm 1$ ,  $48 \pm 2$  and  $180 \pm 10$  °C, respectively.<sup>7, 25</sup> PHBs have major limitations in their mechanical properties and their susceptibility to degrade under high temperature and shear processing conditions.<sup>26</sup>

By contrast, the second polymer used in this study is a random copolymer composed of repeating units with pentyl- and propyl-side-chains named poly[(3-*R*-hydroxyoctanoate)-*co*-(3-*R*-hydroxyhexanoate)], referred to as PHOHHx. The incorporation of repeating units with larger chain-length in PHA (co)polymers by bacterial synthesis, allows for a new generation

of PHAs with improved thermomechanical properties. PHOHHx properties are remarkably different than those of PHB, showing a lower degree of crystallinity, and lower melting points as determined by DSC ( $T_g \approx -35$  °C, and  $T_m = 60 \pm 10$  °C).<sup>27</sup>

The degradation of PHAs is affected by several factors including their side-chain length, crystallinity, and the composition of the degrading medium. We hypothesize that the interdependency of these factors can be studied by controlling the degradation conditions and the polymer state at the air-water interface. In a first step, the solvent quality, the packing density and the state (semi-crystalline, amorphous) of PHB and PHOHHx were determined at different pHs, by means of Langmuir monolayer isotherms and Polarization Modulation Infrared reflection-absorption spectroscopy (PM-IRRAS). Then, the influence of the side-chains and the polymers' crystallinity on the material abiotic degradation was assessed by LMD experiments. The degradation curves of the amorphous films were fit to quantitative models for the hydrolytic degradation of polyesters. PHB monolayers were prepared with different crystallinity (10%, 30% and 40%) to investigate the effect on the degradation behavior of the material. The influence of degradation on the mechanical properties of the films was studied *in situ* using interfacial shear rheology.

## **MATERIALS AND METHODS**

### **Biopolymer synthesis and characterization**

PHOHHx hetero-oligomer was synthesized by bacterial fermentation at shaken flask level using *Pseudomonas putida* KT2440 and 15 mM of octanoic acid as carbon source. PHOHHx production medium, culture conditions, polymer purification and characterization have been described in our previous publications.<sup>28, 29</sup> PHOHHx co-monomer molar ratio was previously determined as 94% 3-*R*-hydroxyoctanoate – 3HO, and 6% 3-*R*-hydroxyhexanoate – 3HHx by

methanolysis and HPLC. PHB homo-oligomer was obtained from GoodFellow (#BU391150). The number average of molecular weight ( $M_n$ ) was determined by multidetector Gel Permeation Chromatography as described before,<sup>30</sup> using chloroform as eluent with a flow rate of 1 ml/min at 35 °C, and 0.2 wt % toluene as internal standard. Molecular weights were determined in universal calibration using Polystyrene standards. For PHOHHx,  $M_n = 37\,800$  g/mol  $\pm$  10% with a polydispersity index (PDI) of  $2.0 \pm 0.1$ , which is accepted as a low PDI value for (co)polymers produced by bacteria.<sup>31</sup> For PHB,  $M_n = 160\,000$  g/mol  $\pm$  10% with a PDI of  $3.6 \pm 0.1$ .

### **Surface pressure vs. area ( $\pi$ - $A$ ) isotherms**

$\pi$ - $A$  isotherms were recorded on a polytetrafluoroethylene Langmuir trough (high compression trough with a surface area of  $A = 550$  cm<sup>2</sup>, KSV NIMA, Finland) equipped with Delrin barriers, for controlling the mean molecular area (MMA), and a level compensation system (KSV LTD, Finland). The MMA for PHOHHx and PHB was calculated based on the average weight and the molar fraction of the repeating units (3HB, 3HO and 3HHx) and the surface area of the trough during compression. The changes in the surface tension of the A–W interface (surface pressure), after spreading the (co)polymer from a chloroform solution, were monitored by a Wilhelmy plate microbalance. Before an experiment was started, the chloroform was allowed to evaporate for 10 min. The final concentration at the interface was  $C_f = 0.04$   $\mu$ g/ml. The Langmuir layers were laterally compressed at constant compression rates of 10 mm/min. The temperature of the subphase for PHOHHx and PHB isotherms was kept constant at  $22 \pm 0.5$  °C.  $\pi$ - $A$  isotherms were repeated at least two times. All presented isotherm data correspond to individual experiment data reproducible with a random measurement error of  $\approx 5\%$  concerning the surface pressure or the MMA values for the independently repeated experiments.

## Langmuir Monolayer Degradation (LMD) experiments

Degradation experiments were carried out using the high compression trough setup explained above. The (co)polymer films at the A–W interface ( $C_f = 0.04 \mu\text{g/ml}$ ) were compressed to the degradation surface pressure  $\pi_D$  with a compression rate of 10 mm/min. Hydrolytic degradation of PHA films was tested in subphases consisting of i) phosphate-buffered saline (PBS, pH = 7.4), and ii) KOH (pH = 10-13). The surface pressure was held constant at  $\pi_D = 12 \text{ mN/m}$ . Further experiments to evaluate changes in the mechanical properties/crystallinity of PHA films were performed at surface pressure  $\pi = 12 \text{ mN/m}$  or  $18 \text{ mN/m}$ . LMD and crystallization experiments were coupled to an interfacial rheology system. Initially, the layers were compressed and held at  $\pi = 12$  or  $18 \text{ mN/m}$  on a MilliQ water subphase (pH = 6). After  $\approx 200$  min the compression was paused, and the pH of the subphase was adjusted to pH = 12.3 or pH = 13 by injection of 10 M KOH (Merck, ultrapure). The pH of the subphase was detected to decrease quite fast, in absence of the polymer layer, when pH >12, most probably due to dissolution of carbon dioxide forming carbonic acid.

## Rheology Experiments

Rheology experiments at the A–W interface were carried out with an Interfacial Shear Rheometer (IRS, model MCR502) from Anton Paar (Austria), which consists of a biconical disk coupled to a driving motor, and to a torque and normal force transducer unit. The edge of the bicone is placed in the interface. The bicone had a radius of  $r = 25.5 \text{ mm}$ . The angle of its tip was  $166.8^\circ$ . Measurements were carried out at defined strain of 8% (assuming an edge-wall distance of 3.5 mm when a circular cap is used) and an oscillation frequency of  $\omega = 0.1 \text{ rad/s}$ . For degradation experiments, the distance between bicone and trough edge was set to 100 mm

when calculating the interfacial moduli using the algorithm from the Rheocompass software. The spread volume for rheology degradation/crystallization experiments was doubled to obtain a final concentration of  $C_f = 0.08 \mu\text{g/ml}$ , considering that the area available for the monolayer was lower due to the bicone ( $530 \text{ cm}^2$ ). An algorithm implemented in the Rheocompass software was used to convert the measured bulk properties into interfacial values. The dynamic moduli were recorded as a function of time and polymer surface pressure. The storage modulus ( $G'$ ) accounts for the elastic component, and the loss modulus ( $G''$ ) for the viscous component of the response to oscillatory shear. The analysis of the crystallization and degradation behavior was based on the complex interfacial viscosity  $|\eta_s^*|$  as the relevant parameter describing the viscoelastic response, with  $\eta_s^* = \eta_s' - i\eta_s'' = \frac{G_s'}{\omega} - i\frac{G_s''}{\omega}$ .<sup>32</sup>

### ***In situ* PM-IRRAS measurements**

Infrared reflection-absorption spectroscopy (IRRAS) was used to detect crystallization in PHA films. Measurements were carried out with a PM-IRRAS spectrometer (Biolin Scientific, Espoo, Finland) coupled to a medium size trough ( $A = 243 \text{ cm}^2$ ) from the same company. The IR-beam was focused onto the A–W surface. The photoelastic modulator was set to achieve a phase shift between p and s-polarized light of  $\frac{\lambda}{2}$  at  $2900 \text{ cm}^{-1}$ . The angle of incidence was set to  $74^\circ$ . The integration time was 500 s. The differential reflectivity spectrum  $S$  is calculated from the collected difference ( $\Delta R$ ) and sum spectra ( $\Sigma R$ ) of the detected intensities of the p- and s- polarized light as  $S = \frac{\Delta R}{\Sigma R} = \frac{R_s - R_p}{R_s + R_p}$ . To obtain the spectrum of the film adsorbing to the A–W interface, the sample spectrum is normalized with respect to the spectrum of the bare A–W interface  $S_0$  with  $S_{film} = \frac{S - S_0}{S_0}$ . A sample spectrum calculated in this way is very sensitive to fluctuations of the reference spectrum. Therefore,  $N$  reference spectra were recorded until

the normalized differential intensity spectrum between the last two spectra was a flat line between  $3000\text{ cm}^{-1}$  and  $1200\text{ cm}^{-1}$ .

## Results

### 1. Influence of pH on the chain conformation of PHA monolayers

The interest in the degradation of PHAs has led to the evaluation of their degradability in different environmental and physiological-like conditions of variable pH, temperature and microbial composition. Abiotic hydrolysis of PHB and PHOHHx (co)polyesters under physiological-like pH (PBS, pH = 7.4) is expected to be an extremely slow process. Moreover, it was previously found that hydrolytic and enzymatically catalyzed degradation of PHA by extracellular e-PHA depolymerase enzymes occur at alkaline pH.<sup>33-36</sup> With the aim of conducting abiotic degradation experiments at elevated pH, the influence of pH on the chain conformation and the crystallization behavior of the polymer was studied.

The compression isotherms of PHOHHx and PHB films were recorded at neutral and elevated pH. The crystallization of PHB was followed by means of PM-IRRAS and interfacial shear rheology. For both (co)polymers, compression isotherms showed a strong dependence on pH, with the slope becoming more gradual under alkaline conditions (Figure 1). Such a gradual slope hints at more extended chain conformations due to better solvent quality.<sup>37</sup> The solvent quality is an important aspect when using Langmuir monolayers as a model system to study the degradation behavior of macromolecules. It is implied that chains, which are in a semi-dilute state under good solvent conditions at the A–W interface, contain much more water than they would in bulk, resulting in strongly accelerated hydrolysis. On the other hand, if chains are in bad or theta solvent condition and in the concentrated regime, they contain less

water and hydrolysis kinetics are expected to be more in line with their bulk behavior. The selection of the degradation conditions, in particular the degradation surface pressure ( $\pi_D$ ), should therefore be based on an analysis of the compression isotherm. In the semi-dilute state, the surface pressure  $\pi$  of polymer monolayers depends on the areal concentration of repeating units  $\Gamma$  according to  $\pi \sim \Gamma^y$ , where  $\Gamma = \frac{1}{MMA}$ .<sup>38</sup> The semi-dilute regime can be identified as a linear region from a double logarithmic plot of surface pressure vs. MMA, and the exponent  $y$  is obtained as the negative slope (see Figure 1). The exponent  $y$  is related to the 2D Flory exponent ( $\nu$ ) via  $y = \frac{2\nu}{2\nu-1}$  and signifies the solvent quality. For good solvents,  $\nu = \frac{3}{d+2}$ , with  $d$  being the dimensionality; therefore, in two dimensions  $\nu = \frac{3}{4} = 0.75$ . As for poor solvents in two dimensions,  $\nu = \frac{1}{2} = 0.5$ .<sup>37, 39</sup>

At neutral pH, PHOHHx is in poor solvent conditions at the air–water interface, with  $\nu = 0.53$  at pH = 7.5. The solvent quality increases with pH, with a calculated Flory exponent of  $\nu = 0.63$  at pH = 13. The transition from semi-dilute to concentrated regime is observed at  $\pi^{**} = 1.8$  mN/m at pH=7.4 and  $\pi^{**} = 11.7$  mN/m at pH = 13. For the presumably less hydrophobic PHB, the solvent quality of the A–W interface is better, with  $\nu = 0.68$  at pH = 7.5 and  $\nu = 0.81$  at pH = 12. The transition from semi-dilute to concentrated regime shifts from  $\pi^{**} = 6$  mN/m at pH= 7.4 to  $\pi^{**} = 7.6$  mN/m at pH = 12. At higher pH, degradation of PHB is so fast that an analysis of the compression isotherm is not carried out. For consistency, all monolayer degradation experiments were performed at a surface pressure of  $\pi_D = 7.5$  mN/m. That means that degradation at pH < 12 was carried out in the concentrated regime for both (co)polymers while degradation at pH > 12 took place in the semi-dilute regime. PHB was in good solvent conditions while PHOHHx was in poor solvent conditions.

The isotherms of PHOHHx and PHB both show a distinct kink at pH = 7.4 (Figure 1). The kink is blurred and shifts to higher surface pressure when the pH is increased. Brewster angle

microscopy images of the PHOHHx layer show a sudden appearance of a great number of bright spots when the layer is compressed over the kink.<sup>3</sup> For PHOHHx at pH = 7.4, the surface pressure cannot increase further after the kink, indicating that the layer undergoes a 2D->3D transition. In contrast, at pH = 12.3, the surface pressure can be increased beyond the kink. The surface pressure remains stable when compression is halted; suggesting that removal of chain segments from the A–W interface requires energy even beyond the 2D->3D transition.

For PHB, the surface pressure increases upon compression beyond the kink, but drops rapidly when compression is stopped. The increasing surface pressure results from a finite compression rate, i.e. the compression rate exceeds the rate of the 2D->3D transition. When compression is halted, the surface pressure relaxes to about 9 mN/m. Assuming that the relaxation of the surface pressure is caused by a 2D to 3D transition, there needs to be a source of energy that counteracts the energetic penalty for uncovering the A–W interface.

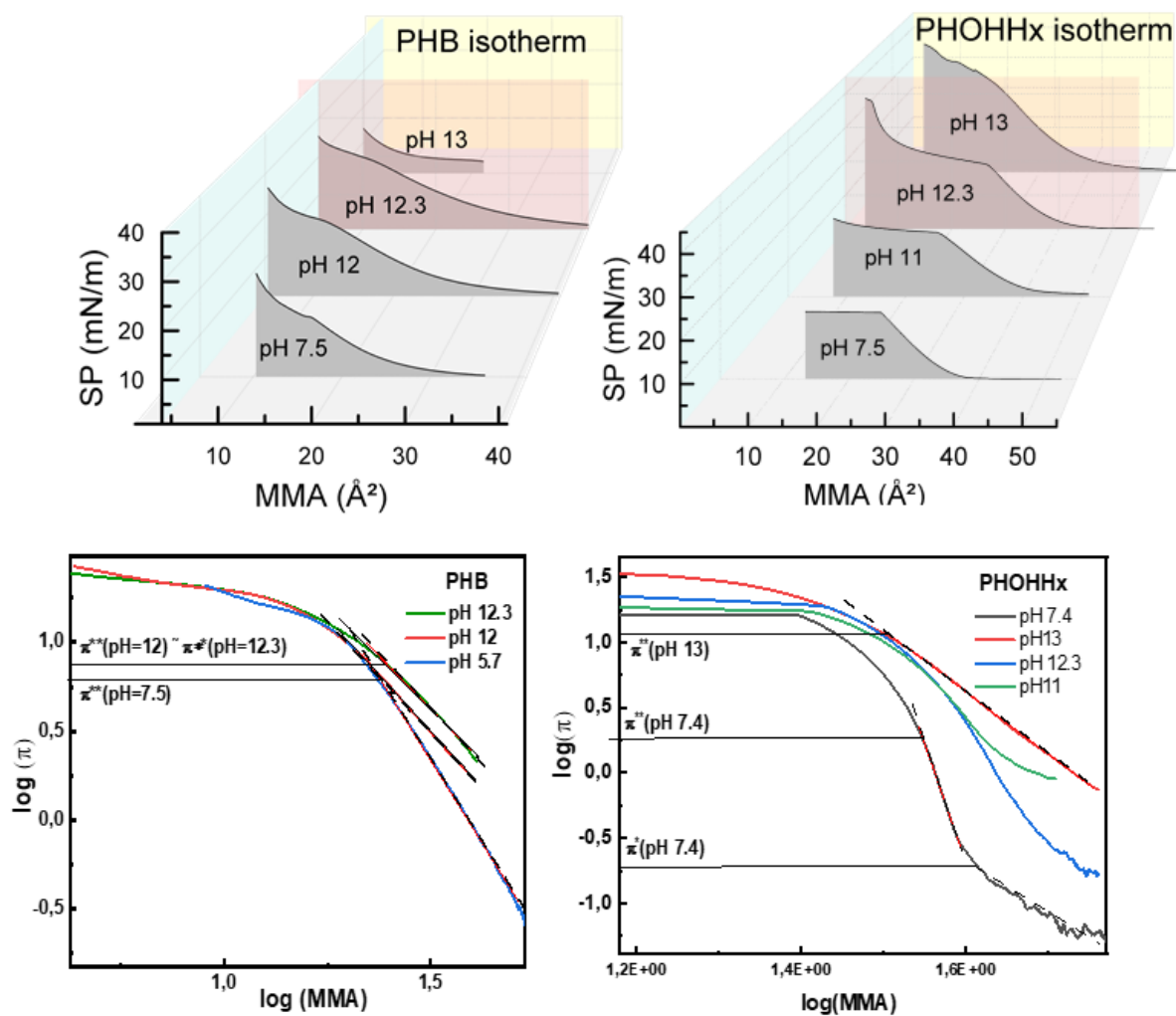


**Figure 1. Top:** Compression isotherms obtained for PHB and PHOHHx monolayers. **Bottom:** Double logarithmic plot of surface pressure vs. mean molecular area (MMA). The surface pressure  $\pi^{**}$  for the transition from the semi-dilute to the concentrated state increases with pH. The exponent  $y$  is obtained by a linear fit to the curves between  $\pi^{**}$  and  $\pi^{*}$ . The transition from dilute to semi-dilute regime at  $\pi^{*}$  is only observed under poor solvent conditions. The starting concentration was relatively high, meaning that the chains were already overlapping after spreading when under good solvent conditions.

Previous studies of PHB monolayers, including IR spectroscopy at the A–W interface, found that the 2D to 3D transition is accompanied by crystallization.<sup>40</sup> Clearly, such a phase transition

can provide the energy for removing chain segments from the A–W interface. These previous studies are in line with PM-IRRAS spectra of PHB at the A–W interface (KOH, pH = 10), which were recorded at different surface pressures below  $\pi = 12$  mN/m, and for 2 h time-lapse at  $\pi = 12$  mN/m. Figure 2 shows the normalized PM-IRRAS spectra between 1200 and 2000  $\text{cm}^{-1}$ . The carbonyl stretching absorption at  $\approx 1722$   $\text{cm}^{-1}$ , which is the strongest IR signal in bulk PHB, is very faint below  $\pi = 12$  mN/m. The reason for the weak signal is that PM-IRRAS only observes bonds with a preferential orientation relative to the A–W interface. When polymer chains are in a random coil conformation, the orientation of the functional groups is statistical, and no net PM-IRRAS signal is observed. In contrast, when the layer is withheld at  $\pi = 12$  mN/m, the carbonyl stretching band starts to grow and become relatively sharp. The crystallization hypothesis is supported by the absence of a carbonyl stretching band in PHOHHx, even when compressing the (co)polymer well beyond the 2D->3D transition, as presented in our previous publication.<sup>3</sup>

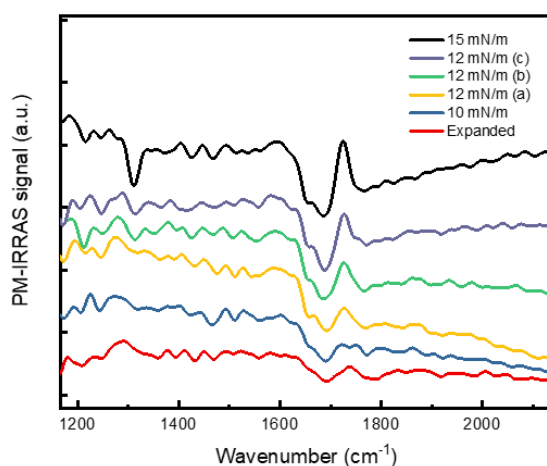


**Figure 2.** PM-IRRAS spectra of PHB at different surface pressures. The spectra at  $\pi = 12$  mN/m were recorded 15 min after the surface pressure was reached (a), 45 min after the surface pressure was reached (b) and 150 min after the surface pressure was reached (c). The spectrum at  $\pi = 15$  mN/m was recorded after compressing the same layer further.

Further evidence to the hypothesis of compression-induced crystallization of PHB is provided by *in situ* interfacial shear rheology (Figure 3A). Below the kink in the compression isotherm, the dynamic interfacial moduli could not be distinguished from the bare A–W interface with our bicone measurement geometry. When the layer was compressed above the transition point, a sharp increase of the moduli was observed. When the pH was increased to pH = 12, the kink in the isotherm shifted to higher surface pressures, and so did the step-like appearance of the interfacial moduli. In contrast, the interfacial moduli of the longer side-chain PHOHHx could not be distinguished from the bare A–W interface below and above the transition surface pressure (Figure 3B). The sudden increase of the dynamic moduli therefore distinguishes the onset of crystallization, from a monolayer collapse without crystallization. The absence of crystallization of PHOHHx is in line with the low crystallinity and low melting point of these (co)polymers in bulk.<sup>25,41,42</sup> The DSC curves of our sample showed an endothermic peak during the initial heating (Figure S1. supporting information), but no crystallization in the second cooling cycle. If the polymer is able to crystallize at all, it does so extremely slowly and to a low extent.

Under the hypothesis that the areal concentration of the repeating units at the A–W interface determines the surface pressure, the relative area reduction during isobaric crystallization is identical to the fraction of the layer that extends into the third dimension. Thus, the degree of crystallinity should be close to the relative area reduction. This conclusion is in line with the film area vs. time curve during isobaric crystallization. The sigmoid shape is typical for evolution of the crystalline volume fraction during isothermal polymer crystallization (Figure 3C). In bulk polymers, the driving force for crystallization is related to supercooling. In a compressed monolayer, the surface pressure provides an additional driving force. The equilibrium surface pressure where PHB crystals neither form nor melt at neutral pH is  $\approx 9$

mN/m. The further the layer is compressed beyond the surface pressure, the more it moves out of equilibrium and therefore, the higher the driving force for crystallization.

From these experiments, it can be concluded that for  $\text{pH} < 10$ , PHA is under rather bad solvent conditions at the air-water interface and does not contain too much water, especially at higher packing density. These conditions are somewhat similar to the conditions found in degrading bulk materials. The crystallinity of semi-crystalline PHB Langmuir films could be adjusted by means of surface pressure, with interfacial shear rheology providing the means to study the interplay between crystallinity, degradation and dynamic mechanical properties of PHB.

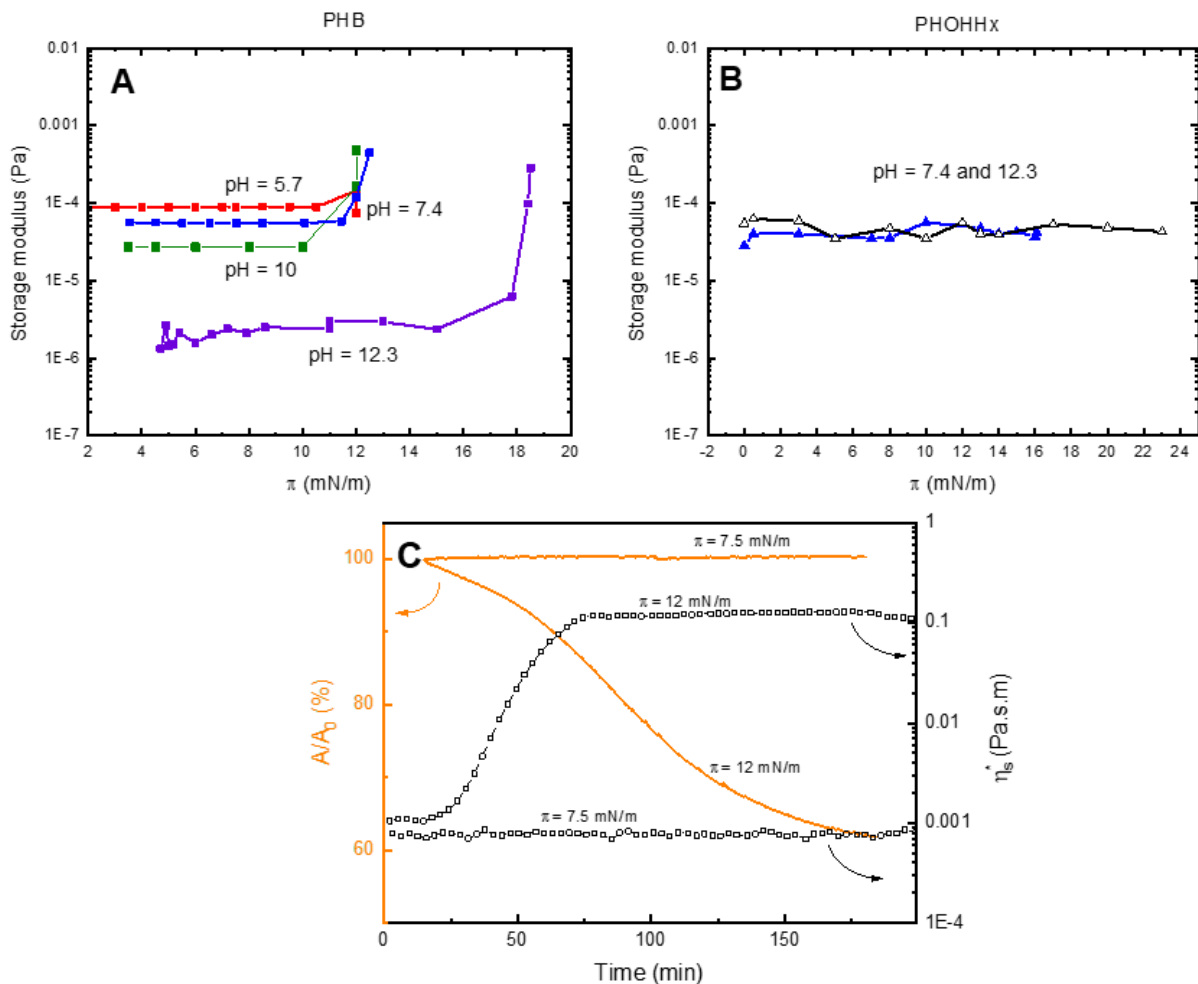


**Figure 3:** A) Dynamic moduli of PHB in dependence on surface pressure during compression at different pH. B) Dynamic moduli of PHOHHx in dependence on surface pressure during compression at neutral and high pH. C) Time dependence of complex interfacial viscosity at constant surface pressure below ( $\pi = 7.5$  mN/m) and at the transition surface pressure (12 mN/m). MMA as a function of time (solid lines). Complex interfacial viscosity  $\eta_s^*$  as a function of time (open squares).

## 2. Influence of side-chain length on hydrolytic degradation of PHA

Hydrolysis and thermal decomposition are the main degradation mechanisms expected for the investigated (co)polymers in the absence of biological agents. Since the labile bond in the main-chain is the ester bond, hydroxide ions are suitable catalysts for the decomposition of PHA (Figure 4). Studying the abiotic degradation of PHA Langmuir films in dependence on pH will allow the generation of a model to define and compare the impact of phase morphology and side-chain length on the degradation mechanism and kinetics of PHA.

The hydrolysis of PHOHHx hetero-polymer (pentyl/propyl group as side-chain) and PHB homo-polymer (methyl group as side-chain) was studied at physiological-like conditions (PBS, pH = 7.4) and elevated pH ranging from 10 to 13, at constant surface pressure  $\pi_D = 7.5$  mN/m, below the phase transition observed for PHB in  $\pi$ - $A$  isotherms. By studying the degradation of both polymers in the amorphous state, we rule out the effect of crystallinity. The Langmuir degradation curves of PHB and PHOHHx in Figure 5 display the change in area ratio ( $A/A_0$ ) occupied by the PHA monolayer as a function of time at a constant surface pressure. In neutral/mild-alkaline conditions, the area occupied per molecule was unchanged over a period of 16 h for both (co)polymers. This underlines the slow degradation of these polyesters at

physiological-like conditions in the absence of PHA degrading enzymes, which has been reported by other authors, specifically for PHB and its copolymers.<sup>43-45</sup>

PHOHHx and PHB hydrolysis was then induced using KOH solutions to identify the effect of the side-chain on the degradation kinetics of PHA. Prior to this study, both scenarios have been observed, where the relatively amorphous PHOHHx would degrade i) quicker<sup>46, 47</sup> or ii) slower<sup>48, 49</sup> than the short side-chain length PHB as the most crystalline member of the PHA family. In a more controlled study, where the authors simulated different managed and unmanaged environments, PHB was found to degrade faster and in more conditions than PHO homopolymer. The latter failed to degrade in 6 of the 7 scenarios tested.<sup>10</sup> However, these studies were performed under enzymatic catalysis. Their results are hard to compare due to the difference in the experimental conditions, e.g. the microorganism distribution and therefore the distribution of depolymerase enzymes in soils. In addition, the phase morphology and sequence structure of the specific polymer samples was certainly not identical.

Here, by studying amorphous monolayers, we rule out all effects of geometry or phase morphology. At  $\pi_D = 7.5$  mN/m both (co)polymers are amorphous (Figure 4). Up to pH = 12, when PHOHHx is in the concentrated regime and still in relatively bad solvent conditions, it does not show signs of degradation. PHB, which is under good solvent conditions and at the transition between concentrated and semi-dilute regime, undergoes a slight degradation at pH = 12. When the subphase pH was increased to 12.3, PHB was found to be hydrolysable; meanwhile, the area-ratio of PHOHHx monolayers at the same pH was still constant. Then, at pH = 13, degradation proceeded about 200 times faster for PHB than for PHOHHx.

We could conclude that PHOHHx with longer alkyl side-chains degrades slower under alkaline hydrolysis when compared to PHB. This could be attributed to the more hydrophobic side-chains shielding the ester bonds, and reducing the ability of water molecules to

hydrolytically cleave the bonds (Figure 4), as reported for the anhydride bonds of polyesteranhydrides.<sup>50</sup>

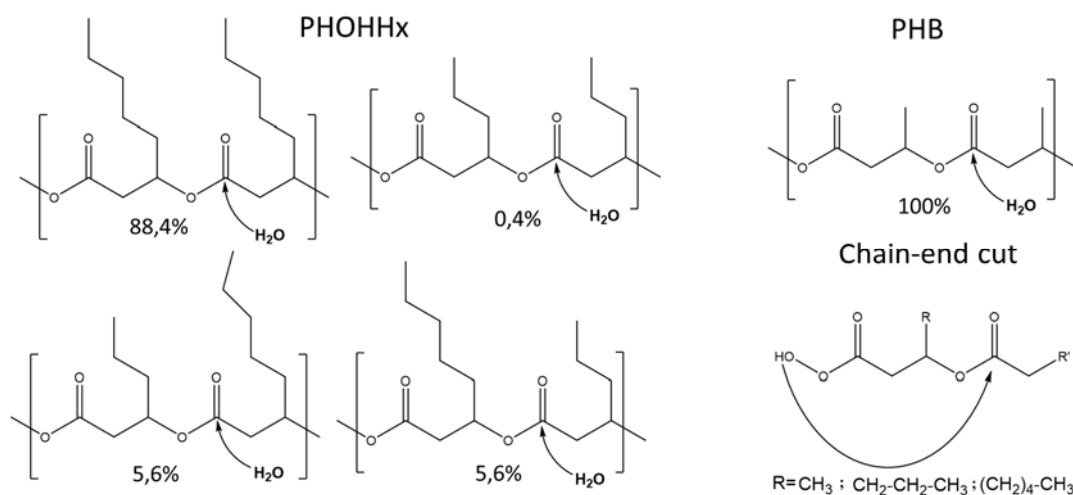


**Figure 4:** Representation of the ester bonds and degradation mechanisms in PHA. For PHOHHx, there are four different diads. The molar fractions are calculated based on statistical probability based on comonomer content. The longer the side-chains in PHOHHx diads, the more steric shielding of the ester bonds against hydrolytic attack is expected. Polymer abiotic degradation from the chain-end can be catalyzed by an intramolecular attack of the chain-ends on an ester bond. Longer side-chains in the chain-end make create steric hindrance for this attack and decrease the reaction rate.

For PHB at pH = 12.3 and PHOHHx at pH = 13, the dissolution profile was nearly identical. After an initial fast degradation, it ceased at around 40% of the (co)polymer mass loss at the interface. This can be explained by a decrease of pH in the subphase from pH = 12.3 or 13 to pH  $\approx$  11, after 5 h, due to dissolution of carbon dioxide forming carbonic acid, slowing down

the hydrolysis of the films as demonstrated by the degradation of PHB at pH = 12.3 performed in a sealed trough with permanent argon circulation (Figure S3. supporting information).

### ***Mechanistic consideration***

Recording the change in the polymer monolayer area at isobaric conditions yields the rate of dissolution of the degradation products in the aqueous subphase. The fundamental types of chain-scission, namely random scission and chain-end-scission, can be distinguished based on the characteristic release kinetics of water-soluble degradation fragments.<sup>23</sup> The mechanism of PHA hydrolysis is still not fully clear. The degradation is believed to progress via random scission of ester bonds, formation of insoluble and soluble oligomers, and to finally result in the ultimate degradation products (3-hydroxybutyric acid and crotonic acid, for PHB). This is usually observed in solutions of NaOH (up to 4M) and high temperatures (around 180 °C).<sup>36</sup> <sup>51</sup> However, the  $A/A_0$ -time plot at pH = 12.3 and pH = 13 for PHB and PHOHHx, respectively (Figure 5), are more in line with a chain-end-scission model. The initial degradation rate is very high, which is in contradiction with a random scission process. It is implied that only very short segments of the hydrophobic PHOHHx are water-soluble, while the molecular weight of the (co)polymer is very high. Generation of a meaningful number of water-soluble fragments by random fragmentation therefore takes a certain time for this (co)polymer, resulting in an initial period of slow dissolution. Therefore, the fast initial degradation strongly projects a preferential degradation at the chain-ends. In such a mechanism, one expects faster degradation with decreasing molecular weight of the (co)polymer, since the fraction of chain ends increases compared to the internal repeating units. However, PHB with higher molecular weight degraded faster than PHOHHx at pH = 12.3. Consequently, for PHA (co)polymers in the amorphous state, the length of the side-chain has a bigger impact on the degradation rate than the molecular weight. The shorter side-chain results in better solvent conditions and chain-end degradation is associated with a back-biting mechanism (Figure 4).<sup>52</sup> It is clear that such a

back-folding of the chain on itself is obstructed by long side-chains. For the same reason, it is questionable whether such a mechanism would also occur in a bulk material where the flexibility of the chains is much lower than in a low viscosity Langmuir film. In such a simple model with exclusive degradation at the chain-end, the area reduction rate is given by:

$$\frac{dA}{dt} = -k \quad (1)$$

Where  $k$  is a rate constant, which depends on the number of chain-ends, pH etc. The decrease of the pH due to dissolution of CO<sub>2</sub> is expected to follow first order kinetics with a rate constant  $l$ .

$$\frac{dA}{dt} = -k_0 \exp(-lt) \quad (2)$$

$$A(t) = \frac{k_0}{l} (1 - \exp(-lt)) \quad (3)$$

As can be seen from the fit-curves in Figure 4, the simple model perfectly agrees with the degradation curve of PHOHHx, but is not so successful for PHB. Presumably, in this shorter side-chain polymer, random chain scission is also a factor. This finding underlines the shielding effect of side-chains in PHOHHx. The quantitative models describing a mixed chain scission process are available.<sup>24</sup> However, since the participation of the chain-end is probably not relevant in bulk PHB (see below), they were not applied here.

A long-term PHOHHx degradation experiment performed for 17 days at pH = 7.4 showed no abiotic degradation of the film during the first 9 days. A rather slow decrease in (co)polymer area was observed in the following 3 days, which corresponds to a mass loss of the PHOHHx (co)polymer film of about 12%. No further degradation was observed up to the 17<sup>th</sup> day (Figure S2. supporting information). This experiment gives insight into the long-term hydrolysis of a PHA copolymer, with pentyl and propyl groups as side-chain, at pH = 7.4. There are critical parameters for the degradation of polymers, which cannot be easily foreseen and that might be

affected by accelerated degradation conditions.<sup>53</sup> Our results demonstrate the stability of the measurement system for long-term experiments and the potential of the Langmuir monolayer degradation technique to study the unaccelerated degradation of slowly degrading polymers in general.

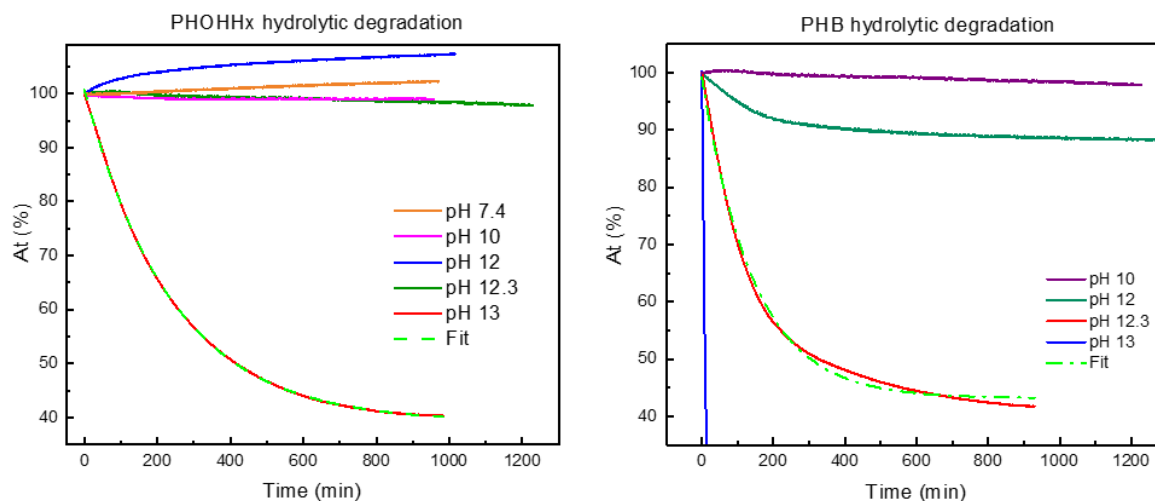


**Figure 5.** PHOHHx and PHB hydrolytic degradation at constant degradation surface pressure of  $\pi_D = 7.5$  mN/m. Fit-curves are shown in green dashed line.

### 3. Influence of polymer state (crystallinity) on hydrolytic degradation of PHA

Water diffusion and hydrolysis of semi-crystalline polymers occur predominately in the amorphous phase.<sup>54</sup> A lower degradation rate is usually expected for polymers with higher crystallinity. PHB is an isotactic homo-polymer whose crystallinity can be controlled at the A-W interface (section 1). This will allow determining the influence of PHB crystallinity on polymer hydrolytic degradation under alkaline conditions. Moreover, by using rheology, we expect to detect changes on the dynamic mechanical properties of the films during degradation. PHB films with different estimated levels of crystallinity were obtained at the A-W interface

(initial subphase, pH = 6) by controlling the surface pressure/molecular area (Figure 6). The PHB solution was spread on a water subphase and compressed to  $\pi_c = 12$  mN/m ( $\approx 10$  and 30% crystallinity) or 18.5 mN/m ( $\approx 40\%$  crystallinity). At that point, when crystallization was induced, the complex interfacial viscosity increased strongly, as seen in section I of Figures 5A and 5B. To obtain  $\approx 30\%$  and  $\approx 40\%$  crystallinity, the films were continuously compressed to maintain the surface pressure constant at 12 or 18.5 mN/m for 2 h, inducing formation and growth of the crystals. To achieve a lower degree of crystallinity of  $\approx 10\%$ , the film was maintained at a constant area per molecule for about 2 h. For all semi-crystalline layers, abiotic degradation was induced in all cases by injection of a concentrated solution of KOH (10 M) to obtain a subphase with a final pH = 12.3 (Figure 6A). From that point, the degradation/crystallization was followed under isobaric conditions. At 10% estimated crystallinity, the amorphous region of the polymer is hydrolyzed in alkaline conditions, causing a decrease in the area per molecule and in the complex interfacial viscosity  $\eta_s^*$ . When the crystallinity of the film is increased to 30%, there is only a slight decrease in the MMA, suggesting a lower availability of amorphous chains for degradation. Nonetheless, the shift in the mechanical properties due to degradation was detectable. In both cases, the decrease in  $\eta_s^*$  upon degradation indicates that hydrolysis has a huge influence on the final viscoelastic properties of the films. Finally, when the film had an estimated crystallinity of 40%, the area reduction was almost zero and only a small decrease of  $\eta_s^*$  was observed, which returns to its maximum after 200 min.

The mass loss from the polymer at the A–W interface, estimated based on the decrease in MMA, was 40%, 15%, and 16%, for the films with 10%, 30% and 40% crystallinity, respectively. Similar observations have been reported for solvent cast films of PHB with different crystallinities (60, 65 and 75%, obtained by annealing at 80, 110, and 140 °C),

subjected to base hydrolysis.<sup>55</sup> This suggests that degradation proceeds mainly in the amorphous phase.

Another noteworthy feature of the degradation behavior in the semi-crystalline state is the different degradation mechanism when compared to the 2D amorphous state. The area vs. time curve has the sigmoidal shape typical of a random scission process,<sup>23</sup> showing a relatively long lag-time with little area loss but significant reduction of the interfacial viscosity (Figures 6A, 6B and 6C).

In a random scission mechanism, under isobaric conditions where the surface pressure is kept constant, it would be expected that the complex interfacial viscosity  $\eta_s^*$  decreases almost instantaneously when the degradation is induced. In comparison, in a chain-end mechanism, the area per molecule should decrease in line with the  $\eta_s^*$ . Unfortunately, as shown in Figure 3A and Figure 6B, when PHB is amorphous state at the A-W interface, the sensitivity of the interfacial rheology setup did not allow distinguishing between the viscosity of bare water and the polymer monolayer.

Due to the low mobility of chain-ends in the semi-crystalline state, random fragmentation is presumably the degradation mechanism of bulk PHB. This finding is in line with the observation that scission of PHB chains occurs at the surfaces and interfaces of lamellar crystals, with formation of unsaturated end groups by dehydration of the chain-ends by  $\beta$ -elimination after ester hydrolysis.<sup>51</sup>

During abiotic degradation at pH = 12.3, we could not detect a chemi-crystallization or secondary crystallization induced by the degradation of the polymer, even at different estimated crystallinities (Figure 6A), as reported for enzymatic degradation of PHB in bulk.<sup>14</sup> However, we realized that the enzymatically catalyzed degradation of PHB is typically much faster than the hydrolytic degradation of the polymer. We applied the conditions for the most efficient hydrolysis of PHB to validate our observation, which was shown in our previous experiments

to be  $\text{pH} = 13$  (Figure 5). The experiment was performed at 30% estimated crystallinity and constant  $\pi_D = 12 \text{ mN/m}$  as described above. During the stabilization of the system at constant surface pressure  $\pi = 12 \text{ mN/m}$  (Section I in Figure 6A and 6C), before the injection of KOH, the crystallization kinetics follows an S-shape or sigmoidal profile, described by the Avrami equation.<sup>56</sup> The S-shape starts with an initial slow crystallization rate, which results from the time required for a significant number of nuclei to form and grow; followed by a rapid transformation that reaches a boundary where growth stops. The remaining untransformed amorphous phase at the A–W interface is then attacked by the hydroxyl ions, causing an immediate decrease in interfacial viscosity due to cutting of tie-chains between crystallites. The drop in  $\eta_s^*$  occurred in a similar manner as the previous experiments at 10% and 30% crystallization (20% mass loss after 100 min). After 100 min the  $\eta_s^*$  increased again, indicating further nucleation and/or growth of crystals induced by hydrolysis (chemi-crystallization). Furthermore, the  $\eta_s^*$  values seem to decrease for a second time, which could point to an attack of the hydroxyl ions to the amorphous phase within the crystallites or the crystallites themselves at these very alkaline conditions (Figure 6C, Section III). These features agree well with previous findings on semi-crystalline poly(*L*-lactide), where a selective degradation of amorphous regions led to differences of degradation rates in amorphous and crystalline domains.<sup>57</sup> Interestingly, the same authors found a degradation induced crystallization in initially amorphous PLA samples, which was not the case for PHB that remained amorphous with a basal  $\eta_s^*$  values up to total degradation (Figure 6B), even after biotic degradation by depolymerases enzymes (data not shown).

As shown in this section, PHAs in amorphous state are hydrolytically degraded by a chain-end-scission mechanism. The degradation rate decreases strongly with increased crystallinity, affecting the degradability of PHB. Under harsh hydrolysis conditions, a chemi-crystallization of PHB is induced. It should be taken into consideration that lipases have been reported to

degrade some PHAs. Hence, a chemi-crystallization process is expected to occur in implanted PHA-based materials with medium to high crystallinity. None of the (co)polymers used in this work were degraded by lipases, isolated from *Pseudomonas cepacia* or *Rhizopus Oryzae*, in Langmuir degradation experiments. In future research, a model of PHA enzymatic degradation will be developed using specific PHOHHx and PHB depolymerases.

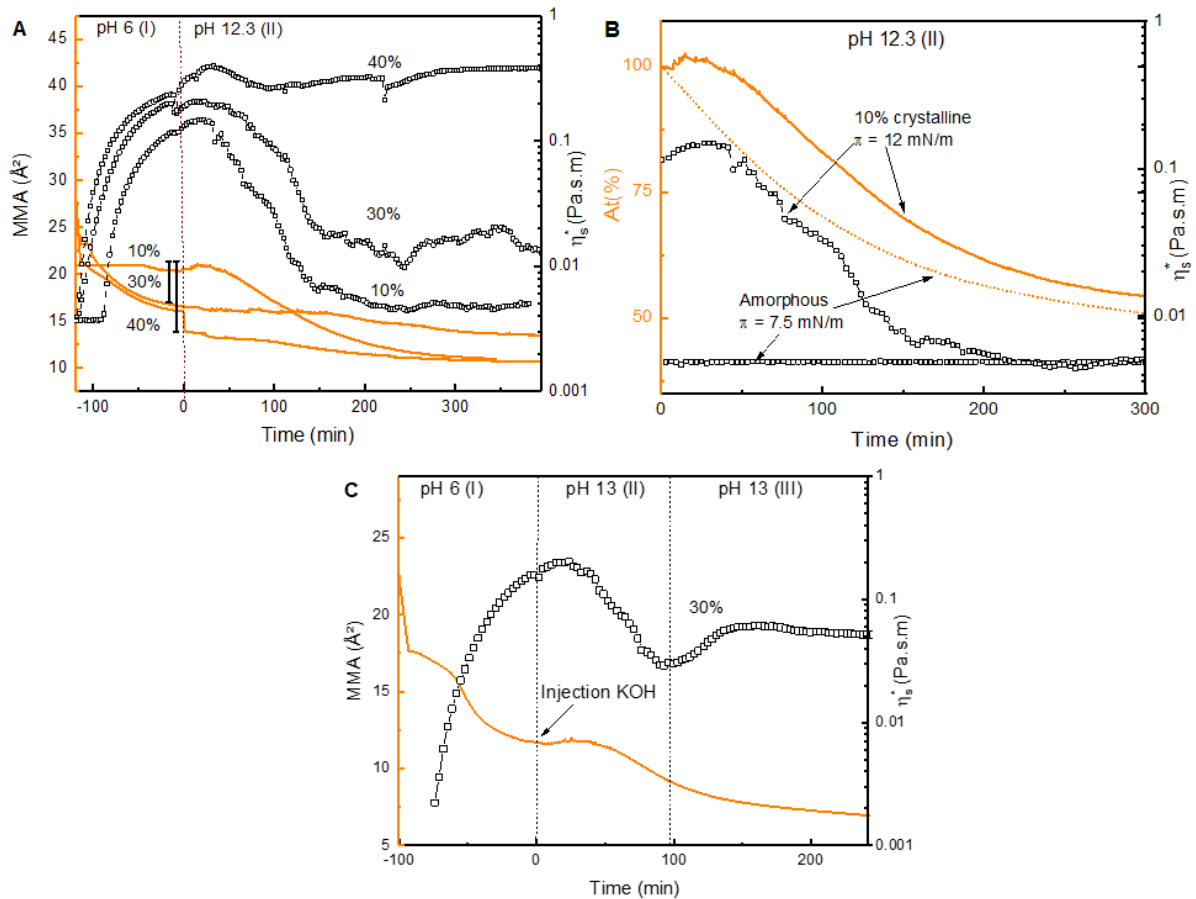


**Figure 6.** A) Degradation/crystallization of PHB at pH = 12.3. MMA ( $\text{\AA}^2$ , solid lines) and complex interfacial viscosity ( $\eta_s^*$ , open squares) as a function of time. Three estimated crystallization levels (10, 30, 40%) were tested. The arrows in 30% and 40% indicate the reduction in area before injection of KOH. B) Relative degradation  $At$  (%) in orange, and complex interfacial viscosity ( $\eta_s^*$ , open squares) as a function of time for 10% crystalline PHB (solid line, taken from figure 6A) and amorphous PHB (dashed line) at pH = 12.3. C)

Degradation/crystallization at 30% estimated crystallization. MMA as a function of time (orange line). Complex interfacial viscosity  $\eta_s^*$  as a function of time (open squares).

Altogether, this paper argues that amorphous PHA made of repeating units with short side-chain (methyl groups) are more easily hydrolyzed under alkaline conditions. Under alkaline conditions, the hydrolysis of PHA follows a chain end-cut mechanism. This mechanism would make the production by the cells of small soluble fragments, for the biosynthesis of new biomolecules, quick and efficient. Surprisingly, PHA degradation catalyzed by specific depolymerases is expected to be more in line with a random degradation mechanism, which requires longer times and more cuts for small fragments to be formed. This assumption will be addressed in future studies. The phase morphology of PHB films is of high relevance for their degradation behavior. In general, the maximum crystallinity for a PHB film to be efficiently degraded up to pH 12.3 was found to be 40%. When the polymer had an initial crystallinity of around 30%, it became between 30% less degradable under alkaline catalysis. In addition, we could infer that semi-crystalline PHA exhibit a secondary chemi-crystallization process upon degradation.

## CONCLUSIONS

A reliable prediction of the degradation behavior of prospective biomaterials by Langmuir monolayers as predictable models requires degradation studies until the very end, as well as consideration of the chemi-crystallization phenomenon. Even under very harsh conditions (pH = 12.3), chemi-crystallization of PHB lead to termination of degradation. The sequence structure and phase morphology of PHA play a key role in the hydrolytic degradation of the polymer films. The high stability of these polymers against hydrolysis highlights the

importance of generating innovative PHAs with improved phase morphology, by introducing repeating units that allow the cleavage of weak ester bonds, but prevent crystallization of the material. Finally, this work supports the Langmuir monolayer technique to closely simulate real-time degradation of polymers under a variety of conditions.

## ACKNOWLEDGMENTS

This work was financially supported by the Helmholtz Association through programme-oriented funding. The authors especially thank Ing. Manuela Keller for support with the presented measurements. We thank Dr. Burkhard Schulz and Prof. M. Auxiliadora Prieto for helpful discussions with Natalia Tarazona during manuscript preparation.

## References

1. Koller, M., Biodegradable and Biocompatible Polyhydroxyalkanoates (PHA): Auspicious Microbial Macromolecules for Pharmaceutical and Therapeutic Applications. *Molecules* **2018**, *23*, (2), 362.
2. Jendrossek, D., Polyhydroxyalkanoate granules are complex subcellular organelles (carbonosomes). *J. Bacteriol.* **2009**, *191*, (10), 3195-202.
3. Tarazona, N. A.; Machatschek, R.; Schulz, B.; Prieto, M. A.; Lendlein, A., Molecular Insights into the Physical Adsorption of Amphiphilic Protein PhaF onto Copolyester Surfaces. *Biomacromolecules* **2019**, *20*, (9), 3242-3252.
4. Mato, A.; Tarazona, N. A.; Hidalgo, A.; Cruz, A.; Jiménez, M.; Pérez-Gil, J.; Prieto, M. A., Interfacial Activity of Phasin PhaF from *Pseudomonas putida* KT2440 at Hydrophobic–Hydrophilic Bionterfaces. *Langmuir* **2019**, *35*, (3), 678-686.

5. Sedlacek, P.; Slaninova, E.; Enev, V.; Koller, M.; Nebesarova, J.; Marova, I.; Hrubanova, K.; Krzyzanek, V.; Samek, O.; Obruca, S., What keeps polyhydroxyalkanoates in bacterial cells amorphous? A derivation from stress exposure experiments. *Appl. Microbiol. Biotechnol.* **2019**, *103*, (4), 1905-1917.
6. Jendrossek, D., Peculiarities of PHA granules preparation and PHA depolymerase activity determination. *Appl. Microbiol. Biotechnol.* **2007**, *74*, (6), 1186.
7. Scandola, M.; Pizzoli, M.; Ceccorulli, G.; Cesaro, A.; Paolletti, S.; Navarini, L., Viscoelastic and thermal properties of bacterial poly (d(-)- $\beta$ -hydroxybutyrate). *Int. J. Biol. Macromol.* **1988**, *10*, (6), 373-377.
8. Rai, R.; Keshavarz, T.; Roether, J. A.; Boccaccini, A. R.; Roy, I., Medium chain length polyhydroxyalkanoates, promising new biomedical materials for the future. *Mater. Sci. Eng: R: Reports* **2011**, *72*, (3), 29-47.
9. Liu, W.; Chen, G.-Q., Production and characterization of medium-chain-length polyhydroxyalkanoate with high 3-hydroxytetradecanoate monomer content by fadB and fadA knockout mutant of *Pseudomonas putida* KT2442. *Appl. Microbiol. Biotechnol.* **2007**, *76*, (5), 1153-1159.
10. Narancic, T.; Verstichel, S.; Reddy Chaganti, S.; Morales-Gamez, L.; Kenny, S. T.; De Wilde, B.; Babu Padamati, R.; O'Connor, K. E., Biodegradable Plastic Blends Create New Possibilities for End-of-Life Management of Plastics but They Are Not a Panacea for Plastic Pollution. *Environ. Sci. Technol.* **2018**, *52*, (18), 10441-10452.
11. Jendrossek, D.; Handrick, R., Microbial degradation of polyhydroxyalkanoates. *Annu. Rev. Microbiol.* **2002**, *56*, (1), 403-432.

12. Newman, J. C.; Verdin, E.,  $\beta$ -hydroxybutyrate: much more than a metabolite. *Diabetes Res. Clin. Pract.* **2014**, *106*, (2), 173-181.
13. Reusch, R. N.; Sparrow, A. W.; Gardiner, J., Transport of poly- $\beta$ -hydroxybutyrate in human plasma. *Biochim. Biophys. Acta, Lipids Lipid. Metab.* **1992**, *1123*, (1), 33-40.
14. Mukai, K.; Doi, Y.; Sema, Y.; Tomita, K., Substrate specificities in hydrolysis of polyhydroxyalkanoates by microbial esterases. *Biotechnol. Lett.* **1993**, *15*, (6), 601-604.
15. Mok, P. S.; Ch'ng, D. H.; Ong, S. P.; Numata, K.; Sudesh, K., Characterization of the depolymerizing activity of commercial lipases and detection of lipase-like activities in animal organ extracts using poly(3-hydroxybutyrate-co-4-hydroxybutyrate) thin film. *AMB Express* **2016**, *6*, (1), 97.
16. Saito, T.; Tomita, K.; Juni, K.; Ooba, K., In vivo and in vitro degradation of poly (3-hydroxybutyrate) in pat. *Biomaterials* **1991**, *12*, (3), 309-312.
17. Freier, T.; Kunze, C.; Nischan, C.; Kramer, S.; Sternberg, K.; Saß, M.; Hopt, U. T.; Schmitz, K.-P., In vitro and in vivo degradation studies for development of a biodegradable patch based on poly(3-hydroxybutyrate). *Biomaterials* **2002**, *23*, (13), 2649-2657.
18. Ying, T. H.; Ishii, D.; Mahara, A.; Murakami, S.; Yamaoka, T.; Sudesh, K.; Samian, R.; Fujita, M.; Maeda, M.; Iwata, T., Scaffolds from electrospun polyhydroxyalkanoate copolymers: fabrication, characterization, bioabsorption and tissue response. *Biomaterials* **2008**, *29*, (10), 1307-1317.
19. Meischel, M.; Eichler, J.; Martinelli, E.; Karr, U.; Weigel, J.; Schmoller, G.; Tschegg, E. K.; Fischerauer, S.; Weinberg, A. M.; Stanzl-Tschegg, S. E., Adhesive strength of bone-

implant interfaces and in-vivo degradation of PHB composites for load-bearing applications. *J. Mech. Behav. Biomed. Mater.* **2016**, *53*, 104-118.

20. Brigham, C. J.; Sinskey, A. J., Applications of polyhydroxyalkanoates in the medical industry. *Int. J. Biotechnol. Wellness Ind.* **2012**, *1*, (1), 52-60.

21. Numata, K.; Abe, H.; Iwata, T., Biodegradability of Poly(hydroxyalkanoate) Materials. *Materials* **2009**, *2*, (3), 1104-1126.

22. Ong, S. Y.; Chee, J. Y.; Sudesh, K., Degradation of Polyhydroxyalkanoate (PHA): a Review. *J. Sib. Fed. Univ. Biol.* **2017**, *10*, 21-225.

23. Machatschek, R.; Schulz, B.; Lendlein, A., Langmuir Monolayers as Tools to Study Biodegradable Polymer Implant Materials. *Macromol. Rapid Commun.* **2019**, *40*, (1), 1800611.

24. Machatschek, R.; Schulz, B.; Lendlein, A., The influence of pH on the molecular degradation mechanism of PLGA. *MRS Advances* **2018**, *3*, (63), 3883-3889.

25. Vahabi, H.; Michely, L.; Moradkhani, G.; Akbari, V.; Cochez, M.; Vagner, C.; Renard, E.; Saeb, M. R.; Langlois, V., Thermal Stability and Flammability Behavior of Poly(3-hydroxybutyrate) (PHB) Based Composites. *Materials (Basel, Switzerland)* **2019**, *12*, (14), 2239.

26. Sudesh, K.; Abe, H.; Doi, Y., Synthesis, structure and properties of polyhydroxyalkanoates: biological polyesters. *Prog. Polym. Sci.* **2000**, *25*, (10), 1503-1555.

27. Song, J. J.; Yoon, S. C.; Yu, S. M.; Lenz, R. W., Differential scanning calorimetric study of poly(3-hydroxyoctanoate) inclusions in bacterial cells. *Int. J. Biol. Macromol.* **1998**, *23*, (3), 165-173.

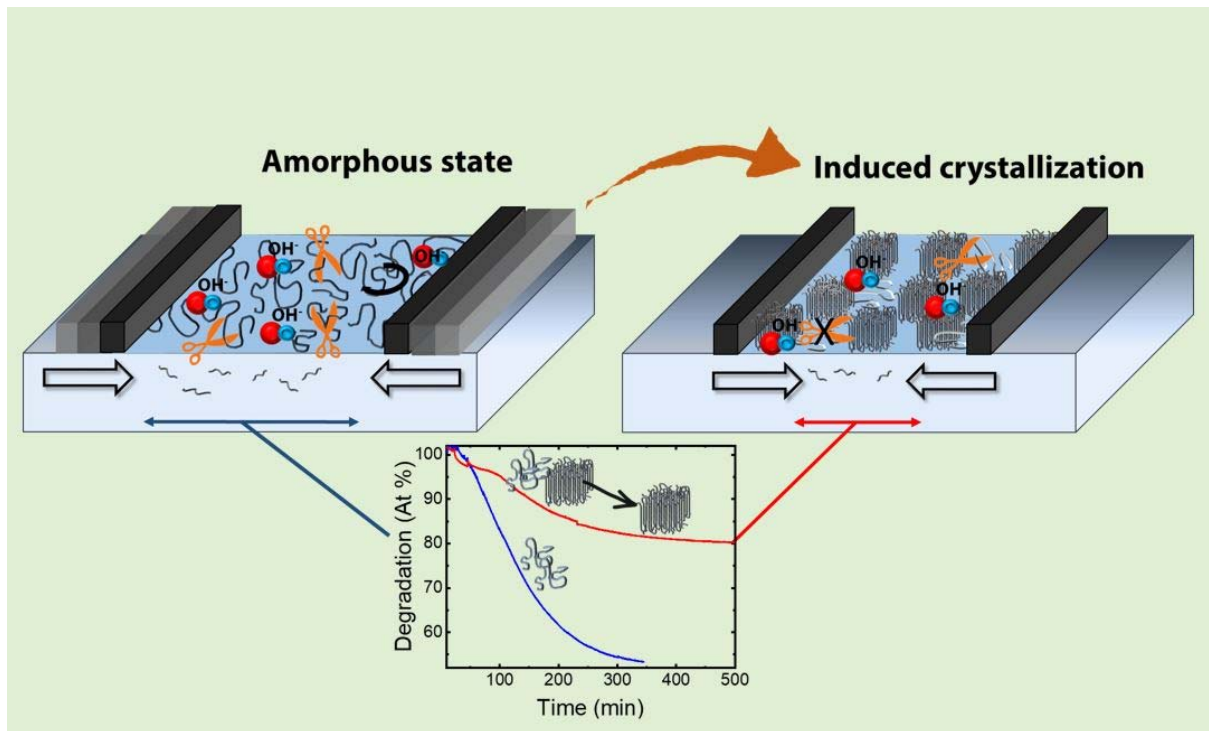
28. Dinjaski, N.; Fernandez-Gutierrez, M.; Selvam, S.; Parra-Ruiz, F. J.; Lehman, S. M.; San Roman, J.; Garcia, E.; Garcia, J. L.; Garcia, A. J.; Prieto, M. A., PHACOS, a functionalized bacterial polyester with bactericidal activity against methicillin-resistant *Staphylococcus aureus*. *Biomaterials* **2014**, *35*, (1), 14-24.
29. Escapa, I. F.; Morales, V.; Martino, V. P.; Pollet, E.; Averous, L.; Garcia, J. L.; Prieto, M. A., Disruption of beta-oxidation pathway in *Pseudomonas putida* KT2442 to produce new functionalized PHAs with thioester groups. *Appl. Microbiol. Biotechnol.* **2011**, *89*, (5), 1583-98.
30. Balk, M.; Behl, M.; Yang, J.; Li, Q.; Wischke, C.; Feng, Y.; Lendlein, A., Design of polycationic micelles by self-assembly of polyethyleneimine functionalized oligo [( $\epsilon$ -caprolactone)-co-glycolide] ABA block copolymers. *Polym. Adv. Technol.* **2017**, *28*, (10), 1278-1284.
31. Chen, G.-Q., Introduction of Bacterial Plastics PHA, PLA, PBS, PE, PTT, and PPP. In *Plastics from bacteria*, Springer: 2010; pp 1-16.
32. Sánchez-Puga, P.; Tajuelo, J.; Pastor, J.; Rubio, M., Dynamic Measurements with the Bicone Interfacial Shear Rheometer: Numerical Bench-Marking of Flow Field-Based Data Processing. *Colloids Interf.* **2018**, *2*, (4), 69.
33. Martinez, V.; de Santos, P. G.; Garcia-Hidalgo, J.; Hormigo, D.; Prieto, M. A.; Arroyo, M.; de la Mata, I., Novel extracellular medium-chain-length polyhydroxyalkanoate depolymerase from *Streptomyces exfoliatus* K10 DSMZ 41693: a promising biocatalyst for the efficient degradation of natural and functionalized mcl-PHAs. *Appl. Microbiol. Biotechnol.* **2015**, *99*, (22), 9605-15.

34. Polyak, P.; Dohovits, E.; Nagy, G. N.; Vertessy, B. G.; Voros, G.; Pukanszky, B., Enzymatic degradation of poly-[(R)-3-hydroxybutyrate]: Mechanism, kinetics, consequences. *Int. J. Biol. Macromol.* **2018**, *112*, 156-162.
35. Foster, L. J. R.; Tighe, B. J., Centrifugally spun polyhydroxybutyrate fibres: accelerated hydrolytic degradation studies. *Polym. Degrad. Stab.* **2005**, *87*, (1), 1-10.
36. Yu, J.; Plackett, D.; Chen, L. X. L., Kinetics and mechanism of the monomeric products from abiotic hydrolysis of poly[(R)-3-hydroxybutyrate] under acidic and alkaline conditions. *Polym. Degrad. Stab.* **2005**, *89*, (2), 289-299.
37. Langevin, D.; Monroy, F., Interfacial rheology of polyelectrolytes and polymer monolayers at the air–water interface. *Curr. Opin. Colloid. Interface. Sci.* **2010**, *15*, (4), 283-293.
38. Maestro, A.; Ortega, F.; Rubio, R. G.; Rubio, M. A.; Kragel, J.; Miller, R., Rheology of poly(methyl methacrylate) Langmuir monolayers: percolation transition to a soft glasslike system. *J. Chem. Phys.* **2011**, *134*, (10), 104704.
39. De Gennes, P.-G.; Gennes, P.-G., *Scaling concepts in polymer physics*. Cornell university press: Ithaca and London, 1979.
40. Lambeek, G.; Vorenkamp, E. J.; Schouten, A. J., Structural Study of Langmuir-Blodgett Mono- and Multilayers of Poly(.beta.-hydroxybutyrate). *Macromolecules* **1995**, *28*, (6), 2023-2032.
41. Marchessault, R. H.; Monasterios, C. J.; Morin, F. G.; Sundararajan, P. R., Chiral poly(beta-hydroxyalkanoates): an adaptable helix influenced by the alkane side-chain. *Int. J. Biol. Macromol.* **1990**, *12*, (2), 158-65.

42. Kim, Y. B.; Lenz, R. W., Polyesters from Microorganisms. In *Biopolyesters*, Babel, W.; Steinbüchel, A., Eds. Springer Berlin Heidelberg: Berlin, Heidelberg, 2001; pp 51-79.
43. Freier, T., Biopolyesters in Tissue Engineering Applications. In *Polymers for Regenerative Medicine*, Werner, C., Ed. Springer Berlin Heidelberg: Berlin, Heidelberg, 2006; pp 1-61.
44. Jo, N.-J.; Iwata, T.; Lim, K. T.; Jung, S.-H.; Lee, W.-K., Degradation behaviors of polyester monolayers at the air/water interface: Alkaline and enzymatic degradations. *Polym. Degrad. Stab.* **2007**, *92*, (7), 1199-1203.
45. Doi, Y.; Kanosawa, Y.; Kawaguchi, Y.; Kunioka, M., Hydrolytic degradation of microbial poly(hydroxyalkanoates). *Makromol. Chem. Rapid. Comm.* **1989**, *10*, (5), 227-230.
46. Schirmer, A.; Jendrossek, D.; Schlegel, H. G., Degradation of poly (3-hydroxyoctanoic acid)[P (3HO)] by bacteria: purification and properties of a P (3HO) depolymerase from *Pseudomonas fluorescens* GK13. *Appl. Environ. Microbiol.* **1993**, *59*, (4), 1220-1227.
47. Foster, L.; Zervas, S.; Lenz, R.; Fuller, R., The biodegradation of poly-3-hydroxyalkanoates, PHAs, with long alkyl substituents by *Pseudomonas maculicola*. *Biodegradation* **1995**, *6*, (1), 67-73.
48. Woolnough, C. A.; Yee, L. H.; Charlton, T.; Foster, L. J. R., Environmental degradation and biofouling of 'green' plastics including short and medium chain length polyhydroxyalkanoates. *Polym. Int.* **2010**, *59*, (5), 658-667.
49. Lim, S.-P.; Gan, S.-N.; Tan, I. K., Degradation of medium-chain-length polyhydroxyalkanoates in tropical forest and mangrove soils. *Appl. Biochem. Biotechnol.* **2005**, *126*, (1), 23.

50. Basu, A.; Domb, A. J., Recent Advances in Polyanhydride Based Biomaterials. *Adv. Mater.* **2018**, *30*, (41), 1706815.
51. Yu, G.-e.; H. Marchessault, R., Characterization of low molecular weight poly( $\beta$ -hydroxybutyrate)s from alkaline and acid hydrolysis. *Polymer* **2000**, *41*, 1087-1098.
52. van Nostrum, C. F.; Veldhuis, T. F. J.; Bos, G. W.; Hennink, W. E., Hydrolytic degradation of oligo(lactic acid): a kinetic and mechanistic study. *Polymer* **2004**, *45*, (20), 6779-6787.
53. Blanco, I., Lifetime Prediction of Polymers: To Bet, or Not to Bet-Is This the Question? *Materials (Basel, Switzerland)* **2018**, *11*, (8), 1383.
54. Zhou, Q.; Xanthos, M., Nanoclay and crystallinity effects on the hydrolytic degradation of polylactides. *Polym. Degrad. Stab.* **2008**, *93*, (8), 1450-1459.
55. Tapadiya, A.; Vasanthan, N., Crystallization and alkaline hydrolysis of poly(3-hydroxybutyrate) films probed by thermal analysis and infrared spectroscopy. *Int. J. Biol. Macromol.* **2017**, *102*, 1130-1137.
56. Avrami, M., Kinetics of Phase Change. I General Theory. *J. Chem Phys* **1939**, *7*, (12), 1103-1112.
57. Li, S. M.; Garreau, H.; Vert, M., Structure-property relationships in the case of the degradation of massive aliphatic poly-( $\alpha$ -hydroxy acids) in aqueous media. *J. Mater. Sci. - Mater. Med.* **1990**, *1*, (3), 123-130.

# TOC graphic



## Supporting Information

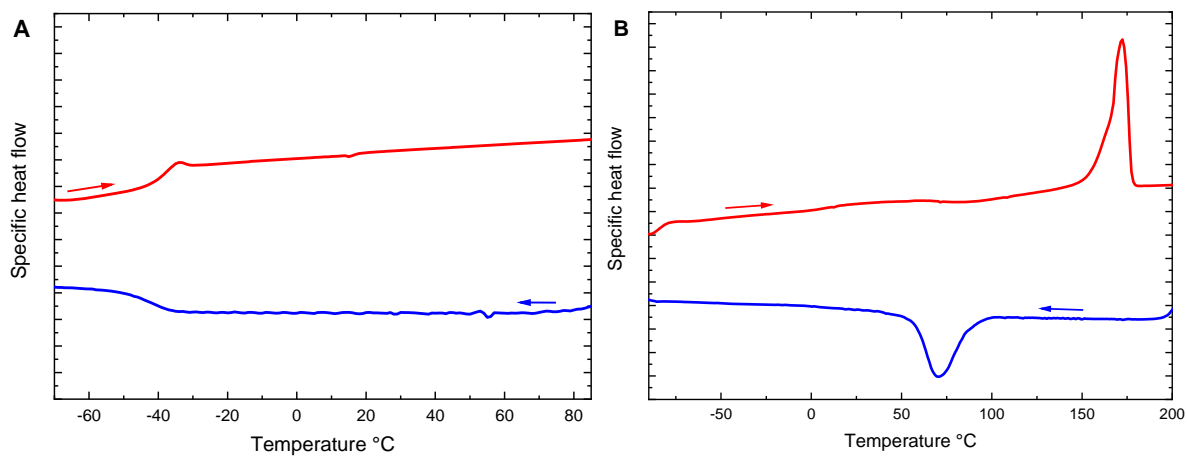


Figure S1. Differential Scanning Calorimetry of PHOHHx (A) and PHB (B). Obtained from second heating (red) and first cooling (blue) run. Cooling rate 10 K/min.

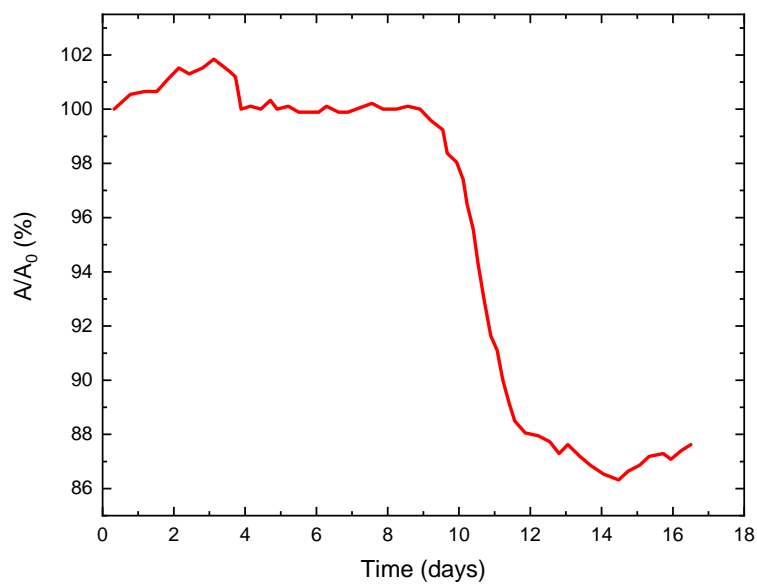


Figure S2. Long-term hydrolytic degradation of PHOHHx at pH 7.4. Decrease in area (%) as a function of time.

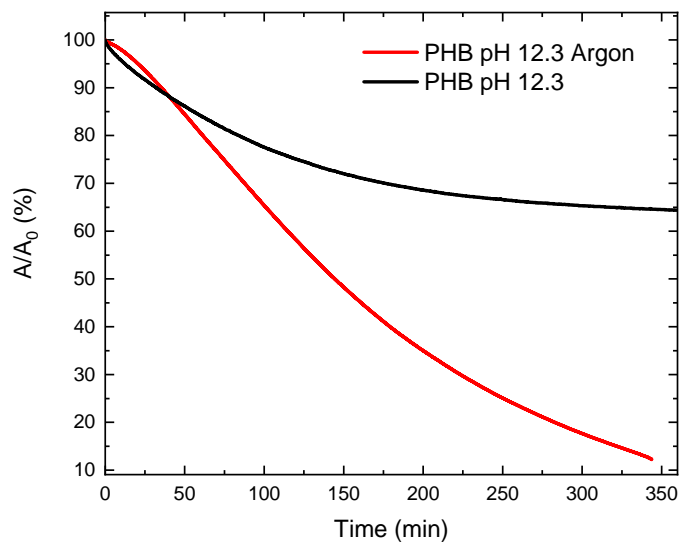


Figure S3. Degradation of PHB at pH 12.3 with (red) and without (black) argon circulation. Decrease in area (%) vs. time plot.